

Geophysical Research Letters®

RESEARCH LETTER

10.1029/2022GL101710

Key Points:

- The relationship between the Pacific Meridional Mode (PMM) and tropical cyclone genesis over the western North Pacific is nonstationary
- The nonstationary relationship stems from the diverse atmospheric responses to PMM that depend on the phase of Pacific Decadal Oscillation

Correspondence to:

C. Wang and B. Wang,
wangchao@nuist.edu.cn;
wangbin@hawaii.edu




Citation:

Wang, C., Fu, M., Wang, B., Wu, L., & Luo, J.-J. (2023). Pacific Decadal Oscillation modulates the relationship between Pacific Meridional Mode and tropical cyclone genesis in the western North Pacific. *Geophysical Research Letters*, 50, e2022GL101710. <https://doi.org/10.1029/2022GL101710>

Received 14 OCT 2022

Accepted 18 FEB 2023

Pacific Decadal Oscillation Modulates the Relationship Between Pacific Meridional Mode and Tropical Cyclone Genesis in the Western North Pacific

Chao Wang^{1,2} , Meiling Fu¹, Bin Wang^{2,3} , Liguang Wu⁴ , and Jing-Jia Luo¹

¹Key Laboratory of Meteorological Disaster of Ministry of Education/Joint International Research Laboratory of Climate and Environment Change/Collaborative Innovation Center on Forecast and Evaluation of Meteorological Disasters, Nanjing University of Information Science and Technology, Nanjing, China, ²Earth System Modeling Center, Nanjing University of Information Science and Technology, Nanjing, China, ³Department of Atmospheric Sciences and International Pacific Research Center, University of Hawaii at Manoa, Honolulu, HI, USA, ⁴Department of Atmospheric and Oceanic Sciences and Institute of Atmospheric Sciences, Fudan University, Shanghai, China

Abstract Pacific Meridional Mode (PMM) is known to be significantly correlated with tropical cyclone (TC) genesis over the western North Pacific (WNP), while the stability of their relationship remains unknown. Here we found that their relationship is nonstationary, which depends on the phase of Pacific Decadal Oscillation (PDO). During the PDO warm phases, the PMM-emanated cyclonic circulation and ascending motion can propagate to the entire WNP due to the enhanced background convection. In contrast, during the PDO cold phases, the PMM-resulted cyclonic circulation and ascending motion are confined to the eastern WNP, while the compensated descending motion prevails in the western WNP. Accordingly, the PMM-induced consistent (inconsistent) changes in large-scale conditions across the western and eastern WNP act to strengthen (weaken) the relationship between the PMM and WNP TC genesis during the PDO warm (cold) phases. The result provides further guidance for improving seasonal prediction of TC genesis.

Plain Language Summary Billions of people in the Pacific islands and Asian coastal regions are subject to enormous tropical cyclone (TC) induced disasters. The Pacific Meridional Mode (PMM), a seasonally evolving mode of coupled climate variability, has a prominent impact on TC genesis in the western North Pacific (WNP) and is usually used as an important predictor for seasonal forecasting of TC genesis. However, stability in the relationship between PMM and TC genesis remains unclear. Here we found that their relationship is nonstationary and depends on the phase of the Pacific Decadal Oscillation (PDO), a decadal fluctuation of the Pacific Ocean. The result highlights the crucial role of PDO in modulating the relationship between the PMM and WNP TC genesis and thus provides further guidance for seasonal forecasting scheme of TC genesis.

1. Introduction

Tropical cyclones (TCs) over the western North Pacific (WNP) bring about enormous disasters to the Pacific islands and coastal regions (Peduzzi et al., 2012; Qin et al., 2023; Q. Zhang et al., 2009). Understanding variations in TC genesis, which largely determine the subsequent track, impact regions and the associated damages, would greatly benefit seasonal forecasting and thus the disaster mitigation for these regions (Camargo, Barnston, et al., 2007; Klotzbach et al., 2019).

Sea surface temperature (SST) anomalies across the tropical and subtropical oceans including the Pacific Ocean, Atlantic Ocean and Indian Ocean, were found to play important roles in variations of the WNP TC genesis (Cai et al., 2023; Camargo, Emanuel, & Sobel, 2007; Chia & Ropelewski, 2002; Du et al., 2011; Huangfu et al., 2018; Huo et al., 2015; Lander, 1994; Magee et al., 2017, 2021; B. Wang & Chan, 2002; C. Wang, Wang, & Wu, 2019; Wu et al., 2020; Zhan et al., 2011; Zhao et al., 2022). C. Wang and Wang (2019) found that the two leading modes of Pacific subtropical high can integrate the trans-basin influences of tropical oceans on the WNP TC activity. For the Pacific sector, while El Niño-Southern Oscillation (ENSO) can shift TC genesis location (Lander, 1994; B. Wang & Chan, 2002), the Pacific Meridional Mode (PMM, Chiang & Vimont, 2004), which is characterized by a warm SST pole elongated in the northeast Pacific Ocean between Hawaii and Baja California and a cool SST pole in the tropical eastern Pacific, tends to modulate the basin-wide TC genesis frequency by emanating

© 2023 The Authors.

This is an open access article under the terms of the [Creative Commons Attribution-NonCommercial License](https://creativecommons.org/licenses/by-nc/4.0/), which permits use, distribution and reproduction in any medium, provided the original work is properly cited and is not used for commercial purposes.

a cyclonic/anti-cyclonic circulation over the WNP (W. Zhang et al., 2016). Moreover, the southwest-northeast oriented SST anomalies associated with the PMM also act as a bridge between the Atlantic SST forcing and the WNP TC activity through air-sea interaction (Ham et al., 2013; Huo et al., 2015; C. Wang et al., 2022).

Since the signal of PMM generally peaks in the boreal winter and spring (Amaya, 2019; Chiang & Vimont, 2004), which leads the TC peak season, it is usually considered as an important predictor of TC genesis for the WNP as well (Cai et al., 2022; C. Wang, Wang, & Wu, 2019; W. Zhang et al., 2017; Q. Zhang, Lai, et al., 2018; X. Zhang, Zhong, et al., 2018). However, C. Wang, Wu, et al. (2019) suggested that the relationship between PMM and TC genesis frequency in the WNP may weaken in the recent two decades, suggesting a possible nonstationary between the PMM and WNP TC genesis. Considering the important role of the PMM in understanding and predicting the WNP TC activity (Gao et al., 2018, 2020; C. Wang, Wu, et al., 2019; W. Zhang et al., 2016), it is of great importance to examine the stationarity of the relationship between the PMM and WNP TC genesis. The present work aims to address the possible nonstationary relationship between the PMM and WNP TC genesis and to explore the possible mechanism.

2. Data and Method

TC observations were obtained from the International Best Track Archive for Climate Stewardship version 4 (IBTrACS, Knapp et al., 2010), which contains six-hourly TC location and intensity records. To minimize the uncertainty among data sources, we used best track data sets from the three operational agencies over the WNP, including the Shanghai Typhoon Institute of China Meteorological Administration (CMA, Ying et al., 2014), the Regional Specialized Meteorological Center of Japan Meteorological Agency (JMA), and the Joint Typhoon Warning Center (JTWC). TCs are defined as those in the data set whose maximum wind speed reaches tropical storm intensity (17.2 m s^{-1}). We focus on the main TC season from May to October. The beginning years of the TC records in CMA, JMA, and JTWC best track data sets are 1945, 1949, and 1951, respectively. Therefore, our analysis period ranges from 1951 to 2019. The reason for using 1951 as the start year is that we want to use as long as possible available data to investigate the stationary of their relationship.

Large-scale parameters were derived from the monthly atmospheric data from the National Centers for Environmental Prediction National Center for Atmospheric Research (NCEP/NCAR) reanalysis (Kalnay et al., 1996) and SST from National Oceanic and Atmospheric Administration Extended Reconstructed SST version 5 (B. Huang et al., 2017). The apparent heating source proposed by Yanai et al. (1973) was used to estimate the anomalous atmospheric heating associated with the PMM.

The dynamical genesis potential index (DGPI) proposed by B. Wang and Murakami (2020) was used to examine the integrated effects of large-scale conditions on TC genesis (B. Wang & Murakami, 2020; C. Wang et al., 2021, 2022). The formulation of the DGPI is as follows:

$$\text{DGPI} = (2 + 0.1V_s)^{-1.7} \left(5.5 - \frac{\partial u}{\partial y} 10^5 \right)^{2.3} (5 - 20\omega)^{3.3} (5.5 + |10^5 \eta|)^{2.4} e^{-11.8} - 1$$

where V_s is the magnitude of the vertical wind shear (m s^{-1}) between 850 and 200 hPa, $\frac{\partial u}{\partial y}$ is the meridional gradient of zonal wind (s^{-1}) at 500 hPa, ω is the 500 hPa vertical pressure velocity (Pa s^{-1}) and η is the absolute vorticity (s^{-1}) at 850 hPa.

3. The Nonstationary Relationship Between PMM and TC Genesis Frequency

TC genesis frequency over the WNP experiences notable inter-annual and decadal variations, which is positively correlated with the PMM index with a correlation coefficient of 0.33 during 1951–2019 (Figure 1a). The correlation is statistically significant but lower than that of W. Zhang et al. (2016) due to the different analysis periods, indicating their relationship may be unstable over the past seven decades. Interestingly, notable inter-decadal variations can be found in their 11-year running correlation coefficients (Figure 1b). A significant positive correlation exists from the late 1970s to the late 1990s but the relationship weakens in the periods before the late 1970s and after the late 1990s. Indeed, two change points around 1978 and 2000 can be identified in the 11-year running correlation coefficients by the sliding t -test. Accordingly, the study period (1951–2019) was divided into three periods (P1:1951–1978, P2:1979–1999, P3:2000–2019) in the following analyses. Particularly, based on the ensemble mean of the three best tracks, their correlation reaches 0.60 during P2, while it drops to 0.22 and 0.26 for P1 and P3, respectively. Note that the nonstationary relationship between the PMM and TC genesis frequency is independent of the adopted best track data. Their correlation coefficient is 0.58/0.58/0.56 during

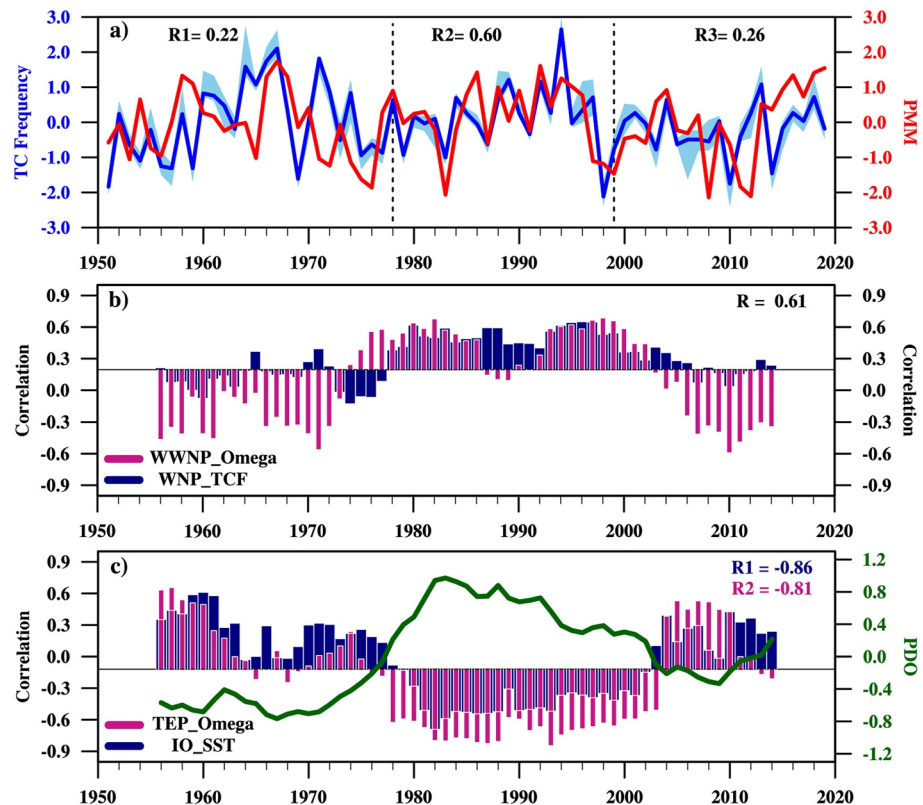


Figure 1. (a) Times series of the Pacific Meridional Mode (PMM) index (red line) and western North Pacific (WNP) tropical cyclone (TC) genesis frequency (blue line) in the TC season (May–October) during 1951–2019. (b) The 11-year running correlation coefficient between the WNP TC genesis frequency (blue bars), 500 hPa Ω over the western WNP (purple bars) and the PMM index during 1951–2019. (c) The 11-year running correlation coefficient between the Indian Ocean SST (blue bars), 500 hPa Ω over the tropical eastern Pacific (purple bars) and the PMM index during 1951–2019. Shadings in (a) denote the standard deviation of TC genesis frequency among the three best track data. The vertical dash lines in (a) separate 1951–2019 into three periods (P1:1951–1978, P2:1979–1999, P3:2000–2019) and $R1$, $R2$ and $R3$ denote the correlation coefficient between blue and red line for the three periods, respectively. R in (b) represents the correlation coefficient between blue and purple bars. The green line in (c) shows the 11-year running mean Pacific Decadal Oscillation (PDO) index, and $R1$ ($R2$) in (c) represents the correlation coefficient between blue (purple) bars and PDO.

P2 based on the CMA/JMA/JTWC data, while it drops to 0.27/0.24/0.11 and 0.26/0.26/0.21 during P1 and P3, respectively. To understand the inter-decadal change in their relationship, in the following analyses we compare the PMM-related large-scale condition anomalies during the three periods.

4. Large-Scale Condition Anomalies and the Driving Mechanism

TC formation requires favorable large-scale conditions (e.g., Emanuel & Nolan, 2004; Gray, 1968; Murakami & Wang, 2010). Here, the DGPI was used to examine the integrated effects of large-scale conditions on TC genesis. Although some differences exist, the regressed spatial pattern of DGPI against the PMM index is generally consistent with that of TC genesis, which shows notable decadal changes (Figures 2a–2f). Since the different DGPI responses to the PMM for the three periods only occur in the western WNP, a DGPI diagnostic analysis, by varying each term in DGPI with the other three terms fixed to their climatology (Camargo, Emanuel, & Sobel, 2007), was conducted in the western WNP. It is found that the vertical motion term is crucial to the opposite DGPI anomalies in the western WNP for the three periods. Subsequently, the 11-year running correlation between the omega over the western WNP and the PMM index shows similar decadal variations to that between the PMM index and TC genesis frequency (Figure 1b). The consistency between the TC genesis and large-scale condition anomalies indicates that changes in the large-scale environments account for the nonstationary relationship between the PMM and WNP TC genesis.

The selected periods based on the PMM–TC genesis relationship interestingly coincide with the negative (P1 and P3) and positive (P2) phases of PDO defined by previous studies (Mantua et al., 1997; Mantua & Hare, 2002;

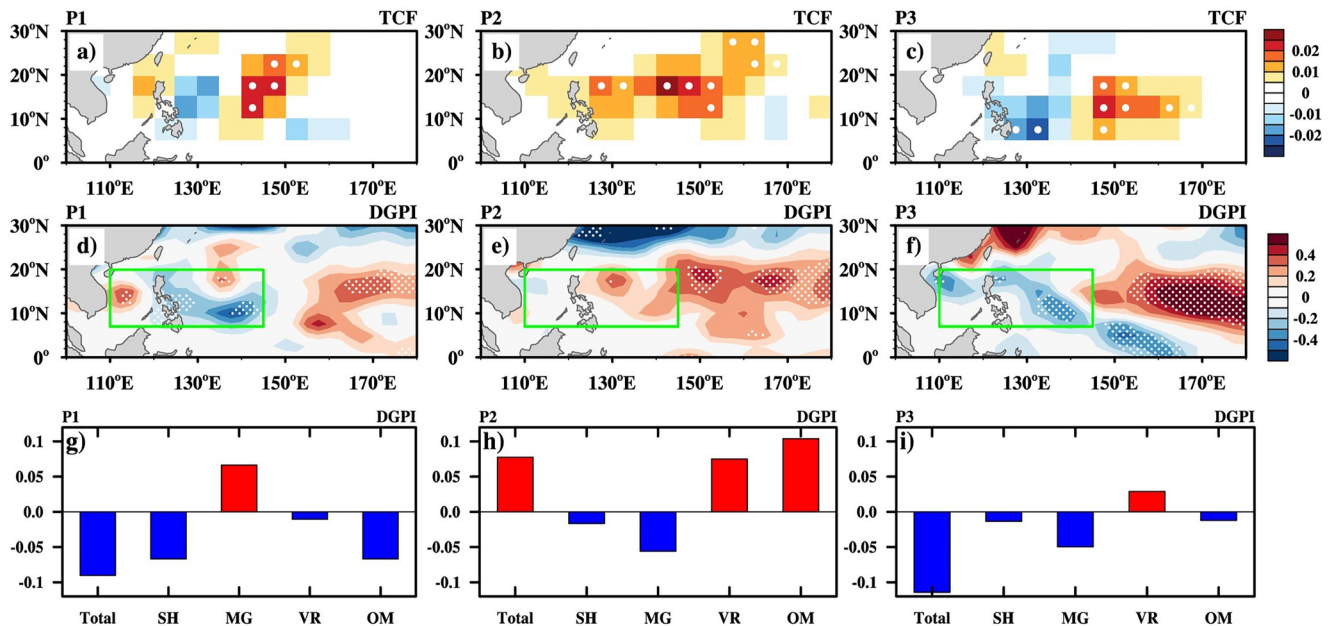


Figure 2. Regressed (a–c) tropical cyclone (TC) genesis density and (d–f) dynamical genesis potential index (DGPI) anomalies against the Pacific Meridional Mode (PMM) index in TC season for the three periods. (g–i) Contributions of the four terms to DGPI anomalies over the western North Pacific (WNP) (7°N–20°N, 110°E–145°E) for the three periods. SH, MG, VR, and OM refers to the DGPI derived from varying vertical wind shear, meridional gradient of 500 hPa zonal wind, 850 hPa absolute vorticity and 500 hPa Ω , respectively, with other variables fixed as climatology. For the total, all four terms in the DGPI are allowed to vary. Green boxes in (d–f) outline the WNP. Dots in (a–f) denote the regressed anomalies that are significant at 90% confidence level.

Newman et al., 2016), suggesting the possible important role of the PDO in the nonstationary relationship of the PMM and WNP TC genesis frequency. During P2, the atmosphere is more sensitive to SST forcing due to the enhanced background convection associated with the positive phase of PDO (Xiang et al., 2013). Accordingly, the PMM-related SST anomalies generate prominent negative convective heating anomalies in the tropical eastern Pacific and positive heating anomalies in the subtropical Northeast Pacific in the boreal winter (December–February, Figure 3b). The resulted winds converge in the tropical central Pacific with positive convective heating anomalies therein, which further emanates a cyclonic circulation as a Rossby response extending to the WNP. Besides the westward migration of PMM-induced positive convective heating, the PMM-initiated ascending motion can be compensated by the descending motions in the tropical eastern Pacific, which would leave space for the westward extension of the PMM-emanated cyclone circulation (Figure 3e). Moreover, the enhanced convective heating in the Maritime continent can stimulate a cyclonic circulation extending to the South Indian Ocean, which acts to accelerate the climatological wind, increase the latent heat flux and cool the SST therein (Figure 3b). The SST cooling can extend to the north Indian Ocean through the wind-induced Ekman feedback and the wind evaporate feedback with the wind reversal to southwest monsoon (Du et al., 2009; Xie et al., 2016), and further maintain into the main TC season through the slowly varying ocean dynamics (Figure 4b). The SST cooling favors the westward extension of the PMM-induced cyclonic circulation by emanating atmospheric Kelvin wave propagating eastward and strengthening the zonal SST gradient across the Indo-Pacific sector (Figure 4b).

In contrast, during P1 and P3 (i.e., negative phases of PDO), the PMM resulted winds converge in the tropical eastern Pacific with the convergence center around 135°W (Figures 3a and 3c) due to the relatively low sensitivity of atmosphere to SST forcing (Xiang et al., 2013), which is located much eastward compared to that during P2 (Figure 3b). As a result, the stimulated anomalous cyclonic circulation shifts eastward and is confined to the eastern WNP (Figures 3a and 3c). Moreover, since the weakened descending motion in the tropical eastern Pacific cannot compensate the PMM-induced ascending motions, remote descending motions occur in the South China Sea and Indian Ocean (Figures 3d and 3f). The associated negative heating anomalies further generate an anti-cyclonic circulation over the Indian Ocean and western WNP (Figures 3a and 3c), which acts to warm the Indian Ocean SST by decreasing the latent heat flux. The SST can further extends to the north Indian Ocean through the Ekman feedback, and maintain to the main TC season (Figures 4a and 4c), favoring the anti-cyclonic circulation and descending motion in the western WNP (Figures 4d and 4f).

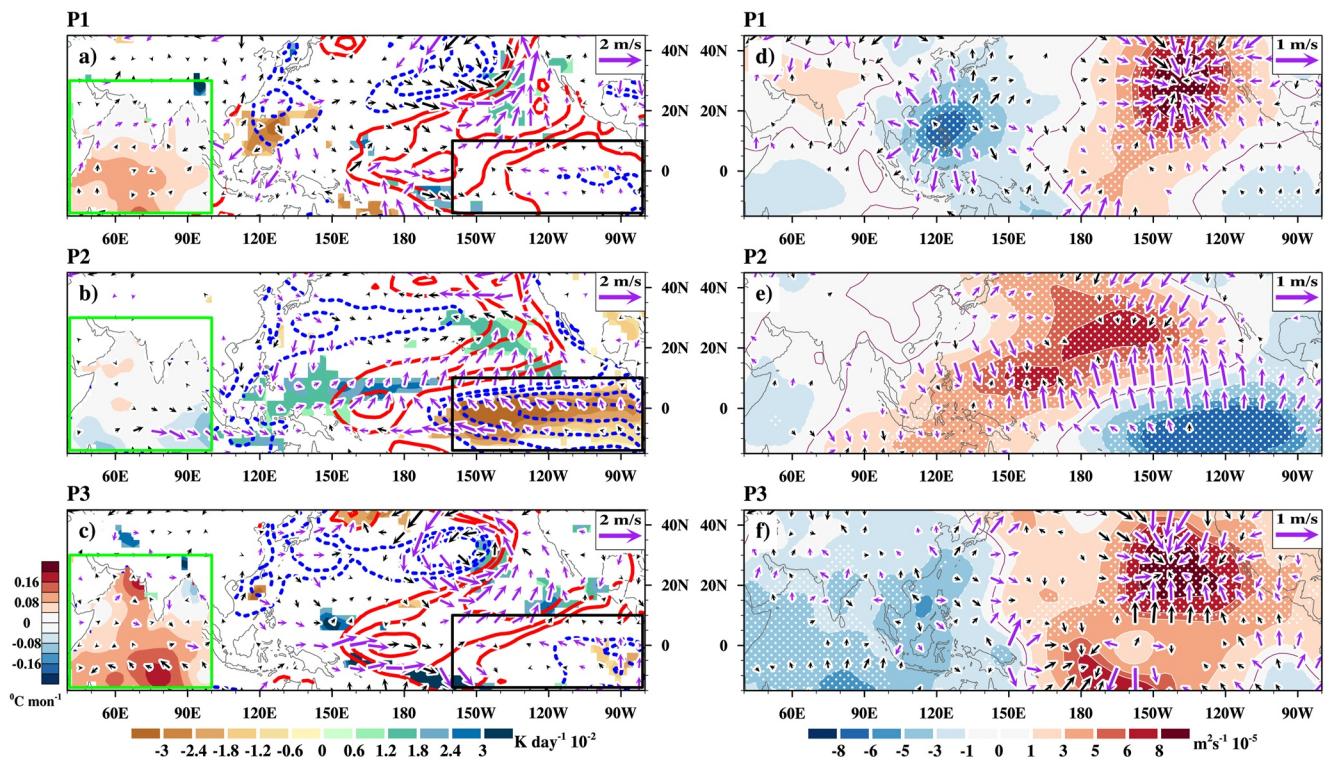


Figure 3. Regressed (a–c) vertically integrated heat source (shadings outside the green box, $\text{K day}^{-1} 10^{-2}$), 1,000 hPa wind (vectors, m s^{-1}), sea surface temperature (SST) (contours, $^{\circ}\text{C}$) and SST tendency (shadings in the green box, $^{\circ}\text{C month}^{-1}$), (d–f) 1,000 hPa velocity potential (shading, $10^{-5} \text{ m}^2 \text{ s}^{-1}$) and divergent wind (vectors, m s^{-1}) anomalies against the Pacific Meridional Mode index in the boreal winter (December–February) for the three periods. Green (black) boxes in (a–c) outline the Indian Ocean (the tropical eastern Pacific). Only the heating anomalies that are significant at 90% confidence level are shown in (a–c). Purple vectors and dots highlight the regressed anomalies that are significant at 90% confidence level.

The results suggest the crucial roles of the diverse response of Indian Ocean SST and vertical motion in the tropical eastern Pacific to the PMM, which depends on the phase of PDO, in the relationship between PMM and large-scale conditions in the WNP. As a result, the 11-year running correlation between the PMM and Indian Ocean (15°S – 25°N , 40°E – 100°E) SST and between the PMM and vertical motion in the tropical eastern Pacific (15°S – 10°N , 150°W – 80°W) show a similar decadal variation to that between the PMM and TC genesis frequency (Figures 1b and 1c). Moreover, both of them are significantly correlated with the PDO index with a correlation coefficient of -0.86 and -0.81 (Figure 1c), highlighting and confirming the crucial role of PDO in the nonstationary relationship between the PMM and WNP TC genesis.

The outputs of Coupled Model Intercomparison Project Phase 6 (CMIP6) historical experiment with Geophysical Fluid Dynamics Laboratory (GFDL) Coupled Model version 4 (GFDL-CM4, Held et al., 2019) were used to confirm the crucial role of PDO in the PMM-related SST and large-scale circulation. During the warm phase of PDO, the PMM-emanated cyclonic circulation can extend westward to the whole WNP with the assistance of Indian Ocean SST cooling and the SST cooling associated descending motion in the tropical eastern Pacific (Figures 5a and 5c). In contrast, during the cold phase of PDO, the Indian Ocean SST warming and the compensated descending motion in the western WNP tend to suppress the westward extension of the PMM-emanated cyclonic circulation to the western WNP (Figures 5b and 5d). Although some biases exist in the simulation, which are resulted from the discrepancies in the simulated PMM features, generally, the numerical experiment reasonably reproduced the anomalous SST and large-scale circulation associated with PMM in different PDO phases, confirming the crucial role of PDO in the nonstationary relationship between the PMM and WNP TC genesis.

5. Summary and Discussion

The PMM is an important driver and predictor for variations of TC genesis in the WNP. Here we found that the relationship between PMM and the WNP TC genesis frequency experiences notable inter-decadal variations.

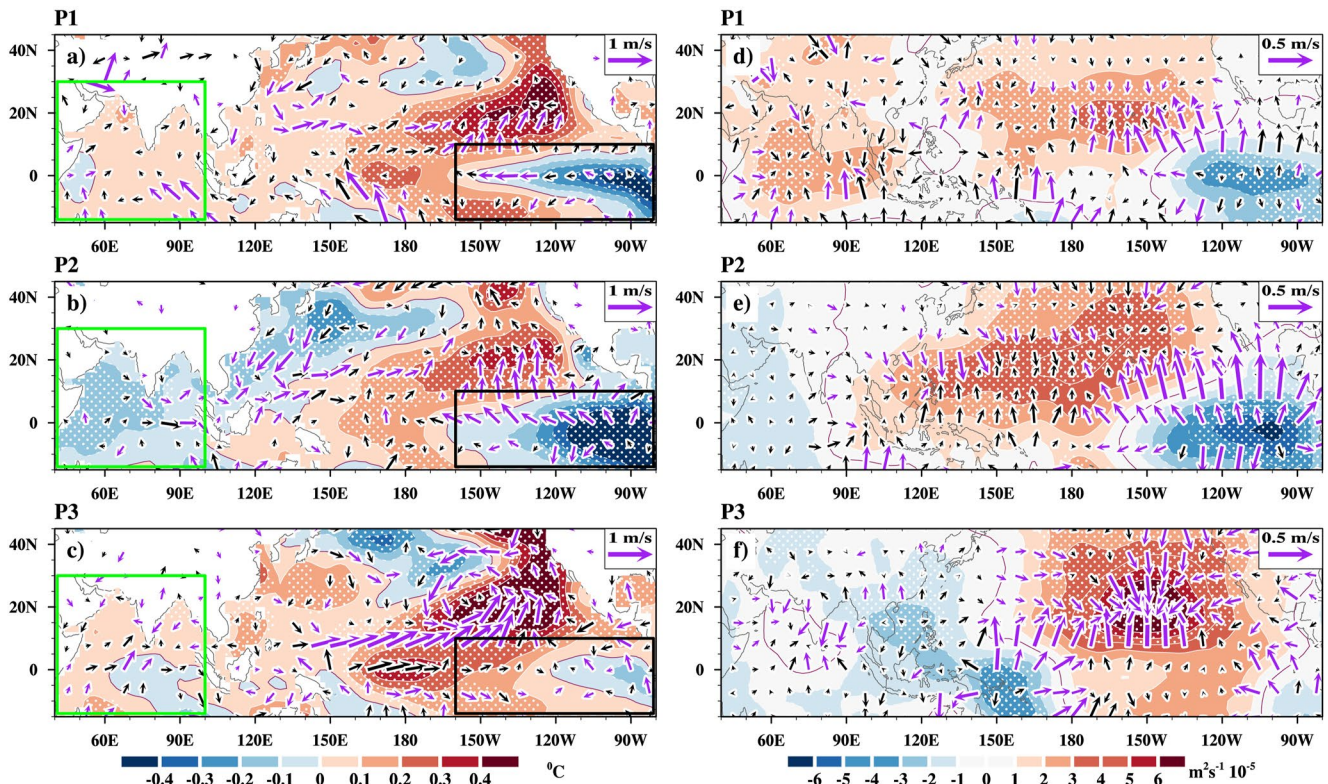


Figure 4. Regressed anomalies in (a–c) sea surface temperature (SST) (shadings, $^{\circ}\text{C}$) and 1,000 hPa wind (vectors, m s^{-1}), (d–f) 1,000 hPa velocity potential (shading, $10^{-5} \text{ m}^2 \text{ s}^{-1}$) and divergent wind (vectors, m s^{-1}) against the Pacific Meridional Mode index in tropical cyclone season for the three periods. Dots (purple vectors) denote the regressed SST (wind) anomalies that are significant at 90% confidence level. Green (black) boxes in (a–c) outline the Indian Ocean (tropical eastern Pacific).

During the study period (1951–2019), significant positive correlations exist from the late-1970s to the late-1990s but the relationship weakens in the periods before the late-1970s and after the late-1990s. This inter-decadal variation is consistent with the PMM-induced diverse large-scale condition anomalies that are dependent on the phase of PDO. During the warm phase of PDO (i.e., P2:1979–1999), the atmosphere is more sensitive to SST forcing than that of the cold phase due to the enhanced background convection. As a result, the PMM SST warming-induced ascending motion and the cyclonic circulation can extend westward to the entire WNP with

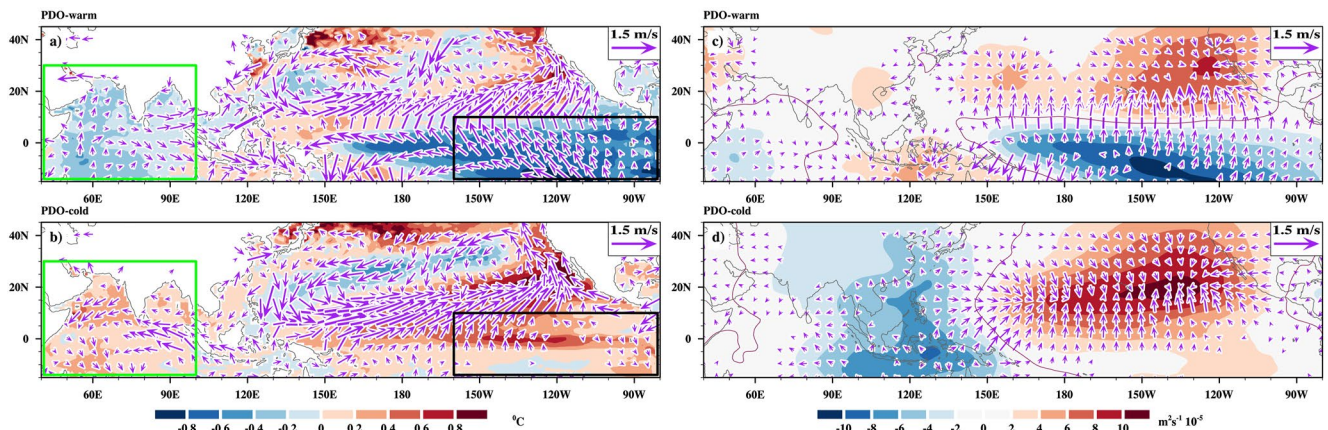


Figure 5. Composite differences in sea surface temperature (SST) (shadings, $^{\circ}\text{C}$) and 1,000 hPa wind (vectors, m s^{-1}) in tropical cyclone (TC) season between positive and negative Pacific Meridional Mode (PMM) years during the (a) warm and (b) cold phases of PDO in the historical experiment of GFDL-CM4. (c and d) same as (a and b) but for 1,000 hPa velocity potential (shading, $10^{-5} \text{ m}^2 \text{ s}^{-1}$) and divergence wind (vectors, m s^{-1}). The green and black boxes in (a and b) outline the Indian Ocean and tropical eastern Pacific. The warm (cold) phases of Pacific Decadal Oscillation (PDO) refers to the period with the 11-year running mean PDO index that are greater than its half standard deviation. The PMM positive (negative) years refers to the year when the PMM index is greater (less) than its half standard deviation.

the assistance of the PMM-initiated Indian ocean SST cooling and the compensation descending motion in the tropical eastern Pacific, leading to the consistent large-scale conditions across the western and eastern WNP, thus contributing to the close relationship between the PMM and WNP TC genesis. In contrast, during the negative phases of PDO (i.e., P1:1951–1978 and P3:2000–2019), the PMM-stimulated anomalous cyclonic circulation shifts eastward and is confined to the eastern WNP due to the relatively weak atmospheric response to the SST forcing. Meanwhile, the PMM-induced remote descending motions prevail in the western WNP and Indian Ocean, which act to warm the Indian Ocean and further lead to an anti-cyclonic circulation over the western WNP and to the opposite large-scale condition anomalies in the western and eastern WNP. The inconsistent large-scale conditions between the western and eastern WNP eventually weaken the relationship between PMM and TC genesis over the WNP. The result highlights the crucial role of PDO phase on the relationship between PMM and TC genesis in the WNP, which suggests that changes in the multi-decadal mean states should be considered when establishing statistical seasonal forecasting models for TC genesis. The result thus provides some new insights for improving seasonal forecasting skill.

While we highlight the role of PDO in modulating the relationship between the PMM and the WNP TC genesis, the own characteristic of PMM may also play some role in the nonstationary relationship. For instance, the magnitude of PMM SST warming increases remarkably during P3, which appeared to be driven by the Atlantic multidecadal oscillation (Yu et al., 2015). The different PMM magnitudes in P1 and P3 may contribute to the different large-scale condition anomalies in the two periods. Moreover, global warming acts to increase the ocean stratification due to the slower warming rate in the ocean subsurface than that of surface waters (P. Huang et al., 2015; Knutson et al., 2001), which can significantly suppress the oceanic vertical mixing and may contribute to the weakened SST cooling over the tropical eastern Pacific in P3. How these factors contribute to the PMM characteristics and how this nonstationary relationship is reproduced in the current state-of-art climate models deserve further explorations.

Data Availability Statement

The International Best Track Archive for Climate Stewardship version 4 data (Knapp et al., 2010) were downloaded at <https://www.ncei.noaa.gov/products/international-best-track-archive?name=ib-v4-access> [Dataset], environmental variables (Kalnay et al., 1996) were obtained from <https://psl.noaa.gov/data/gridded/data.ncep.reanalysis.html> [Dataset], and sea surface temperature (Huang et al., 2017) was downloaded at <https://psl.noaa.gov/data/gridded/data.noaa.ersst.v5.html> [Dataset]. The CMIP6 data (Eyring et al., 2016) were downloaded at <https://esgf-node.llnl.gov/search/cmip6/> [Dataset]. The Pacific Decadal Oscillation (PDO) index (Mantua et al., 1997) was downloaded at <http://research.jisao.washington.edu/data/pdo/> [Dataset], and the Pacific Meridional Mode index (Chiang & Vimont, 2004) was download at <https://www.aos.wisc.edu/~dvimont/MModes/Data.html> [Dataset].

References

- Amaya, D. J. (2019). The Pacific Meridional Mode and ENSO: A review. *Current Climate Change Reports*, 5(4), 296–307. <https://doi.org/10.1007/s40641-019-00142-x>
- Cai, Y., Han, X., Zhao, H., Klotzbach, P. J., Wu, L., Raga, G. B., & Wang, C. (2022). Enhanced predictability of rapidly intensifying tropical cyclones over the western North Pacific associated with snow depth changes over the Tibetan Plateau. *Journal of Climate*, 35(7), 2093–2110. <https://doi.org/10.1175/jcli-d-21-0758.1>
- Cai, Y., Zhao, H., Klotzbach, P. J., Raga, G. B., Xu, J., Wu, L., et al. (2023). Can Tibetan Plateau snow depth influence the interannual association between tropical Indian Ocean sea surface temperatures and rapidly intensifying typhoons? *Journal of Climate*, 1–50. <https://doi.org/10.1175/jcli-d-22-0697.1>
- Camargo, S. J., Barnston, A. G., Klotzbach, P. J., & Landsea, C. W. (2007). Seasonal tropical cyclone forecasts. *World Meteorological Organization Bulletin*, 56(4), 297–309.
- Camargo, S. J., Emanuel, K. A., & Sobel, A. H. (2007). Use of a genesis potential index to diagnose ENSO effects on tropical cyclone genesis. *Journal of Climate*, 20(19), 4819–4834. <https://doi.org/10.1175/JCLI4282.1>
- Chia, H. H., & Ropelewski, C. F. (2002). The interannual variability in the genesis location of tropical cyclones in the northwest Pacific. *Journal of Climate*, 15(20), 2934–2944. [https://doi.org/10.1175/1520-0442\(2002\)015<2934:tivitg>2.0.co;2](https://doi.org/10.1175/1520-0442(2002)015<2934:tivitg>2.0.co;2)
- Chiang, J. C. H., & Vimont, D. J. (2004). Analogous Pacific and Atlantic Meridional Modes of tropical atmosphere – Ocean variability [Dataset]. *Journal of Climate*, 17(21), 4143–4158. <https://doi.org/10.1175/JCLI4953.1>
- Du, Y., Xie, S. P., Huang, G., & Hu, K. (2009). Role of air-sea interaction in the long persistence of El Niño-induced north Indian Ocean warming. *Journal of Climate*, 22(8), 2023–2038. <https://doi.org/10.1175/2008JCLI2590.1>
- Du, Y., Yang, L., & Xie, S.-P. (2011). Tropical Indian Ocean influence on Northwest Pacific tropical cyclones in summer following strong El Niño. *Journal of Climate*, 24(1), 315–322. <https://doi.org/10.1175/2010JCLI3890.1>

Acknowledgments

This study was jointly supported by the National Natural Science Foundation of China (Grant 42088101, 42075031, 41420104002, 41730961 and 41922033). It is the Earth System Modeling Center publication 403 at the Nanjing University of Information Science and Technology. We acknowledge the High-Performance Computer Center of Nanjing University of Information Science and Technology for their support for this work.

- Emanuel, K. A., & Nolan, D. S. (2004). Tropical cyclone activity and the global climate system. In *Preprints, 26th Conference on Hurricanes and Tropical Meteorology* (pp. 240–241). American Meteorological Society.
- Eyring, V., Bony, S., Meehl, G. A., Senior, C. A., Stevens, B., Stouffer, R. J., & Taylor, K. E. (2016). Overview of the Coupled Model Inter-comparison Project Phase 6 (CMIP6) experimental design and organization. *Geoscientific Model Development*, 9(5), 1937–1958. <https://doi.org/10.5194/gmd-9-1937-2016>
- Gao, S., Zhu, L., Zhang, W., & Chen, Z. (2018). Strong modulation of the Pacific Meridional Mode on the occurrence of intense tropical cyclones over the Western North Pacific. *Journal of Climate*, 31(19), 7739–7749. <https://doi.org/10.1175/JCLI-D-17-0833.1>
- Gao, S., Zhu, L., Zhang, W., & Shen, X. (2020). Impact of the Pacific Meridional Mode on landfalling tropical cyclone frequency in China. *Quarterly Journal of the Royal Meteorological Society*, 146(730), 2410–2420. <https://doi.org/10.1002/QJ.3799>
- Gray, W. M. (1968). Global view of the origin of tropical disturbances and storms. *Monthly Weather Review*, 96(10), 669–700. [https://doi.org/10.1175/1520-0493\(1968\)096<0669:gvotoo>2.0.co;2](https://doi.org/10.1175/1520-0493(1968)096<0669:gvotoo>2.0.co;2)
- Ham, Y.-G., Kug, J.-S., Park, J.-Y., & Jin, F.-F. (2013). Sea surface temperature in the north tropical Atlantic as a trigger for El Niño/Southern Oscillation events. *Nature Geoscience*, 6(2), 112–116. <https://doi.org/10.1038/ngeo1686>
- Held, I. M., Guo, H., Adcroft, A., Dunne, J. P., Horowitz, L. W., Krasting, J., et al. (2019). Structure and performance of GFDL's CM4.0 climate model. *Journal of Advances in Modeling Earth Systems*, 11(11), 3691–3727. <https://doi.org/10.1029/2019MS001829>
- Huang, B., Thorne, P. W., Banzon, V. F., Boyer, T., Chepurin, G., Lawrimore, J. H., et al. (2017). Extended Reconstructed Sea Surface Temperature, Version 5 (ERSSTv5): Upgrades, validations, and intercomparisons [Dataset]. *Journal of Climate*, 30(20), 8179–8205. <https://doi.org/10.1175/JCLI-D-16-0836.1>
- Huang, P., Lin, I. I., Chou, C., & Huang, R. H. (2015). Change in ocean subsurface environment to suppress tropical cyclone intensification under global warming. *Nature Communications*, 6(1), 7188. <https://doi.org/10.1038/ncomms8188>
- Huangfu, J., Chen, W., Ma, T., & Huang, R. (2018). Influences of sea surface temperature in the tropical Pacific and Indian Oceans on tropical cyclone genesis over the Western North Pacific in May. *Climate Dynamics*, 51(5–6), 1915–1926. <https://doi.org/10.1007/S00382-017-3989-Y/FIGURES/12>
- Huo, L., Guo, P., Hameed, S. N., & Jin, D. (2015). The role of tropical Atlantic SST anomalies in modulating Western North Pacific tropical cyclone genesis. *Geophysical Research Letters*, 42(7), 2378–2384. <https://doi.org/10.1002/2015GL063184>
- Kalnay, E., Kanamitsu, M., Kistler, R., Collins, W., Deaven, D., Gandin, L., et al. (1996). The NCEP/NCAR 40-year reanalysis project [Dataset]. *Bulletin of the American Meteorological Society*, 77(3), 437–471. [https://doi.org/10.1175/1520-0477\(1996\)077<0437:tnyrp>2.0.co;2](https://doi.org/10.1175/1520-0477(1996)077<0437:tnyrp>2.0.co;2)
- Klotzbach, P., Blake, E., Camp, J., Caron, L.-P., Chan, J. C. L., Kang, N.-Y., et al. (2019). Seasonal tropical cyclone forecasting. *Tropical Cyclone Research and Review*, 8(3), 134–149. <https://doi.org/10.1016/j.tcr.2019.10.003>
- Knapp, K. R., Kruk, M. C., Levinson, D. H., Diamond, H. J., Neumann, C. J., Knapp, K. R., et al. (2010). The International Best Track Archive for Climate Stewardship (IBTrACS) [Dataset]. *Bulletin of the American Meteorological Society*, 91(3), 363–376. <https://doi.org/10.1175/2009BAMS2755.1>
- Knutson, T. R., Tuleya, R. E., Shen, W., & Ginis, I. (2001). Impact of CO₂-induced warming on Hurricane intensities as simulated in a Hurricane model with ocean coupling. *Journal of Climate*, 14(11), 2458–2468. [https://doi.org/10.1175/1520-0442\(2001\)014<2458:IOCIWO>2.0.CO;2](https://doi.org/10.1175/1520-0442(2001)014<2458:IOCIWO>2.0.CO;2)
- Lander, M. A. (1994). An exploratory analysis of the relationship between tropical storm formation in the Western North Pacific and ENSO. *Monthly Weather Review*, 122(4), 636–651. [https://doi.org/10.1175/1520-0493\(1994\)122<0636:AEAOTR>2.0.CO;2](https://doi.org/10.1175/1520-0493(1994)122<0636:AEAOTR>2.0.CO;2)
- Magee, A. D., Kiem, A. S., & Chan, J. C. L. (2021). A new approach for location-specific seasonal outlooks of typhoon and super typhoon frequency across the Western North Pacific region. *Scientific Reports*, 11(1), 1–16. <https://doi.org/10.1038/s41598-021-98329-6>
- Magee, A. D., Verdon-Kidd, D. C., Diamond, H. J., & Kiem, A. S. (2017). Influence of ENSO, ENSO Modoki, and the IPO on tropical cyclogenesis: A spatial analysis of the southwest Pacific region. *International Journal of Climatology*, 37(S1), 1118–1137. <https://doi.org/10.1002/JOC.5070>
- Mantua, N. J., & Hare, S. R. (2002). The Pacific Decadal Oscillation. *Journal of Oceanography*, 58(1), 35–44. <https://doi.org/10.1023/A:1015820616384>
- Mantua, N. J., Hare, S. R., Zhang, Y., Wallace, J. M., & Francis, R. C. (1997). A Pacific interdecadal climate oscillation with impacts on salmon production [Dataset]. *Bulletin of the American Meteorological Society*, 78(6), 1069–1079. [https://doi.org/10.1175/1520-0477\(1997\)078<1069:apicow>2.0.co;2](https://doi.org/10.1175/1520-0477(1997)078<1069:apicow>2.0.co;2)
- Murakami, H., & Wang, B. (2010). Future change of North Atlantic tropical cyclone tracks: Projection by a 20-km-mesh global atmospheric model. *Journal of Climate*, 23(10), 2699–2721. <https://doi.org/10.1175/2010JCLI3338.1>
- Newman, M., Alexander, M. A., Ault, T. R., Cobb, K. M., Deser, C., Di Lorenzo, E., et al. (2016). The Pacific Decadal Oscillation, revisited. *Journal of Climate*, 29(12), 4399–4427. <https://doi.org/10.1175/JCLI-D-15-0508.1>
- Peduzzi, P., Chatenoux, B., Dao, H., De Bono, A., Herold, C., Kossin, J., et al. (2012). Global trends in tropical cyclone risk. *Nature Climate Change*, 2(4), 289–294. <https://doi.org/10.1038/nclimate1410>
- Qin, N., Wu, L., Liu, Q., & Zhou, X. (2023). Driving forces of extreme updrafts associated with convective bursts in the eyewall of a simulated tropical cyclone. *Journal of Geophysical Research: Atmospheres*, e2022JD037061. <https://doi.org/10.1029/2022JD037061>
- Wang, B., & Chan, J. C. L. (2002). How strong ENSO events affect tropical storm activity over the Western North Pacific. *Journal of Climate*, 15(13), 1643–1658. [https://doi.org/10.1175/1520-0442\(2002\)015<1643:HSEETAT>2.0.CO;2](https://doi.org/10.1175/1520-0442(2002)015<1643:HSEETAT>2.0.CO;2)
- Wang, B., & Murakami, H. (2020). Dynamic genesis potential index for diagnosing present-day and future global tropical cyclone Genesis. *Environmental Research Letters*, 15(11), 114008. <https://doi.org/10.1088/1748-9326/abb01>
- Wang, C., & Wang, B. (2019). Tropical cyclone predictability shaped by Western Pacific subtropical high: Integration of trans-basin sea surface temperature effects. *Climate Dynamics*, 53(5–6), 2697–2714. <https://doi.org/10.1007/s00382-019-04651-1>
- Wang, C., Wang, B., & Wu, L. (2019). A region-dependent seasonal forecasting framework for tropical cyclone genesis frequency in the Western North Pacific. *Journal of Climate*, 32(23), 8415–8435. <https://doi.org/10.1175/JCLI-D-19-0006.1>
- Wang, C., Wang, B., Wu, L., & Luo, J.-J. (2022). A seesaw variability in tropical cyclone genesis between the Western North Pacific and the North Atlantic shaped by Atlantic Multidecadal Variability. *Journal of Climate*, 35(8), 2479–2489. <https://doi.org/10.1175/JCLI-D-21-0529.1>
- Wang, C., Wu, K., Wu, L., Zhao, H., & Cao, J. (2021). What caused the unprecedented absence of Western North Pacific tropical cyclones in July 2020? *Geophysical Research Letters*, 48(9), 1–9. <https://doi.org/10.1029/2020GL092282>
- Wang, C., Wu, L., Zhao, H., Cao, J., & Tian, W. (2019). Is there a quiescent typhoon season over the Western North Pacific following a strong El Niño event? *International Journal of Climatology*, 39(1), 61–73. <https://doi.org/10.1002/joc.5782>
- Wu, R., Cao, X., & Yang, Y. (2020). Interdecadal change in the relationship of the Western North Pacific tropical cyclogenesis frequency to tropical Indian and North Atlantic Ocean SST in early 1990s. *Journal of Geophysical Research: Atmospheres*, 125(2). <https://doi.org/10.1029/2019JD031493>

- Xiang, B., Wang, B., Yu, W., & Xu, S. (2013). How can anomalous Western North Pacific Subtropical High intensify in late summer? *Geophysical Research Letters*, 40(10), 2349–2354. <https://doi.org/10.1002/grl.50431>
- Xie, S.-P., Kosaka, Y., Du, Y., Hu, K., Chowdary, J. S., & Huang, G. (2016). Indo-Western Pacific ocean capacitor and coherent climate anomalies in post-ENSO summer: A review. *Advances in Atmospheric Sciences*, 33(4), 411–432. <https://doi.org/10.1007/s00376-015-5192-6>
- Yanai, M., Esbensen, S., & Chu, J.-H. (1973). Determination of bulk properties of tropical cloud clusters from large-scale heat and moisture budgets. *Journal of the Atmospheric Sciences*, 30(4), 611–627. [https://doi.org/10.1175/1520-0469\(1973\)030<0611:DOBPOT>2.0.CO;2](https://doi.org/10.1175/1520-0469(1973)030<0611:DOBPOT>2.0.CO;2)
- Ying, M., Zhang, W., Yu, H., Lu, X., Feng, J., Fan, Y., et al. (2014). An overview of the China Meteorological Administration Tropical Cyclone Database [Dataset]. *Journal of Atmospheric and Oceanic Technology*, 31(2), 287–301. <https://doi.org/10.1175/JTECH-D-12-00119.1>
- Yu, J. Y., Kao, P. K., Paek, H., Hsu, H. H., Hung, C. W., Lu, M. M., & An, S. I. (2015). Linking emergence of the central Pacific El Niño to the Atlantic multidecadal oscillation. *Journal of Climate*, 28(2), 651–662. <https://doi.org/10.1175/JCLI-D-14-00347.1>
- Zhan, R., Wang, Y., & Lei, X. (2011). Contributions of ENSO and East Indian Ocean SSTA to the interannual variability of Northwest Pacific tropical cyclone frequency. *Journal of Climate*, 24(2), 509–521. <https://doi.org/10.1175/2010JCLI3808.1>
- Zhang, Q., Lai, Y., Gu, X., Shi, P., & Singh, V. P. (2018). Tropical cyclonic rainfall in China: Changing properties, seasonality, and causes. *Journal of Geophysical Research: Atmospheres*, 123(9), 4476–4489. <https://doi.org/10.1029/2017JD028119>
- Zhang, Q., Wu, L., & Liu, Q. (2009). Tropical cyclone damages in China 1983–2006. *Bulletin of the American Meteorological Society*, 90(4), 489–496. <https://doi.org/10.1175/2008BAMS2631.1>
- Zhang, W., Vecchi, G. A., Murakami, H., Villarini, G., & Jia, L. (2016). The Pacific Meridional Mode and the occurrence of tropical cyclones in the Western North Pacific. *Journal of Climate*, 29(1), 381–398. <https://doi.org/10.1175/JCLI-D-15-0282.1>
- Zhang, W., Vecchi, G. A., Villarini, G., Murakami, H., Gudgel, R., & Yang, X. (2017). Statistical–dynamical seasonal forecast of Western North Pacific and East Asia landfalling tropical cyclones using the GFDL FLOR coupled climate model. *Journal of Climate*, 30(6), 2209–2232. <https://doi.org/10.1175/jcli-d-16-0487.1>
- Zhang, X., Zhong, S., Wu, Z., & Li, Y. (2018). Seasonal prediction of the typhoon genesis frequency over the Western North Pacific with a Poisson regression model. *Climate Dynamics*, 51(11–12), 4585–4600. <https://doi.org/10.1007/s00382-017-3654-5>
- Zhao, H., Lu, Y., Jiang, X., Klotzbach, P. J., Wu, L., & Cao, J. (2022). A statistical intraseasonal prediction model of extended boreal summer western North Pacific tropical cyclone genesis. *Journal of Climate*, 35(8), 2459–2478. <https://doi.org/10.1175/jcli-d-21-0110.1>